Multiple superconducting states induced by pressure in Mo_3Sb_7

Yejun Feng,[1,2] Yishu Wang,[2] A. Palmer,[3] Ling Li,[4] D. M. Silevitch,[2] S. Calder,[5] and T. F. Rosenbaum[2]
[1]*Okinawa Institute of Science and Technology Graduate University, Onna, Okinawa 904-0495, Japan*
[2]*Division of Physics, Mathematics, and Astronomy, California Institute of Technology, Pasadena, California 91125, USA*
[3]*The James Franck Institute and Department of Physics, The University of Chicago, Chicago, Illinois 60637, USA*
[4]*Department of Materials Science and Engineering, University of Tennessee, Knoxville, Tennessee 37996, USA*
[5]*Quantum Condensed Matter Division, Oak Ridge National Laboratory, Oak Ridge, Tennessee 37831, USA*
(Received 5 August 2016; revised manuscript received 4 January 2017; published 1 March 2017)

Tuning competing ordering mechanisms with hydrostatic pressure in the 4*d* intermetallic compound Mo_3Sb_7 reveals an intricate interplay of structure, magnetism, and superconductivity. Synchrotron x-ray diffraction and magnetic susceptibility measurements, both employing diamond anvil cell technologies, link a first-order structural phase transition to a doubling of the superconducting transition temperature. In contrast to the spin-dimer picture for Mo_3Sb_7, we deduce from x-ray absorption near-edge structure and dc magnetization measurements at ambient pressure that Mo_3Sb_7 should possess only very small, itinerant magnetic moments. The pressure evolution of the superconducting transition temperature strongly suggests its enhancement is due to a difference in the phonon density-of-states with changed crystal symmetry.

DOI: 10.1103/PhysRevB.95.125102

I. INTRODUCTION

The interplay of spin, charge, and lattice degrees of freedom in the 4*d* intermetallic compound Mo_3Sb_7 captures both the excitement and the difficulty of understanding the emergence of collective quantum states. Examples range from metal-insulator transitions [1] to density waves [2] to superconductors [3–8]. In Mo_3Sb_7 itself, superconductivity emerges below a structural phase transition with claims of accompanying magnetic order and spin dimerization [9–11], potentially placing it in a growing cohort of exotic superconductors with unconventional pairing mechanisms [4,12–14].

For both phonon and spin-fluctuation driven superconductivity, the charge or spin couplings between itinerant electrons can be described by the susceptibility, $\chi_{c,m}(\boldsymbol{q},\omega)$, with c and m referring to the charge and magnetic character, respectively, and the excitation modes characterized by momentum $\boldsymbol{q}$ and energy $\hbar\omega$ [4]. While ferromagnetic spin fluctuations suppress phonon-mediated superconductivity, the relationship between antiferromagnetic spin fluctuations and phonon-mediated superconductivity is less transparent. This relationship is a key aspect of the physics of systems such as the cuprates, heavy fermion materials, iron pnictides, organic superconductors, rare-earth borocarbides, and the 3*d* transition-metal compounds CrAs and MnP [3–7,15–18]. Tuning system properties with pressure, chemical doping, and magnetic field can help parse the competing components of $\chi_{c,m}(\boldsymbol{q},\omega)$, both in the collective state itself and across a quantum phase transition.

We combine x-ray diffraction and ac magnetic susceptibility measurements up to 17 GPa of applied pressure to examine the nature of the superconductivity in Mo_3Sb_7. At ambient pressure, Mo_3Sb_7 goes superconducting at $T_c = 2.35$ K, with a structural phase transition from high-temperature cubic symmetry to low-temperature tetragonal symmetry at $T_S = 53$ K [9–11]. Whether this structural transition is magnetically driven is still an open question [9–11,19], although no long-range spin order has been observed to date through either neutron or x-ray magnetic diffraction [11]. Magnetic susceptibility measurements give one $S = 1/2$ local moment per Mo site from fits to a Curie-Weiss law at high temperature [9–11], with spin gap behavior at low temperature that suggests a spin-Peierls transition at T_S [10,11]. The presence of shortened Mo-Mo bond distances in the tetragonal phase [11] reinforces the idea that one-third of the Mo ions form dimers below T_S [10,11]. A valence bond crystal also has been suggested as a possible ground state amid strong spin frustration [9]. The superconductivity has been claimed to be *s* wave at ambient pressure [20–22], but the possibility of unusual magnetic phases at low temperature [9–11,19] have raised the question about the role of spin coupling.

Chemical doping has been exploited previously to study superconductivity in Mo_3Sb_7 [19,23]. We show here that hydrostatic pressure is a particularly effective tuning mechanism, and we find a second superconducting state with a factor of two greater T_c following a pressure-induced first-order phase transition to a higher structural symmetry phase (Fig. 1). The high-pressure phase is cubic and continuously connects to the ambient-pressure, high-temperature paramagnetic phase. By contrast to previous suggestions of spin-dimer magnetic order in a local spin picture [9], we argue that spins in Mo_3Sb_7 should be considered as both highly itinerant and small in magnitude. The link of T_c to structure suggests that spin fluctuations are not a dominant coupling mechanism in this system, while the abrupt variation in T_c points to a symmetry-related difference in the phonon density-of-states.

II. EXPERIMENTAL METHODS AND RESULTS

Mo_3Sb_7 single crystals of several mm in size were grown using a Sb self-flux technique [11]. Single crystals were polished down to plates of 20−30 μm thickness with a surface normal of (1, 0, 0) and broken into small shards ($120 \times 120 \times 20\,\mu m^3$) to be loaded into the diamond anvil cell. The ac magnetic susceptibility measurements at a probe field of 0.5 Oe were carried out using a diamond anvil cell designed for rapidly exploring $H - P - T$ parameter space [24]. Sapphire seats and thermally hardened BeCu or MP35N

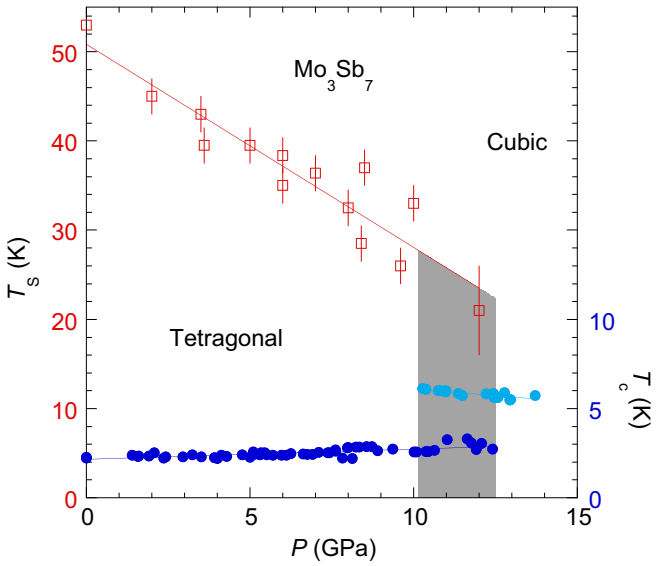

FIG. 1. $P-T$ phase diagram of Mo_3Sb_7. Red squares mark the phase boundary between tetragonal and cubic structures at $T_S(P)$, as determined from electrical resistivity [27]. Superconducting transitions (dark and light blue circles) in both crystal structures are demarcated by characteristic signatures of the magnetic susceptibility. The shaded area marks the phase coexistence region.

gaskets were used to avoid any ferromagnetic background disturbance to the superconducting transition [24,25]. Four different crystals were studied in a methanol:ethanol 4:1 hydrostatic pressure medium. Pressure was monitored by ruby fluorescence *in situ* at low temperature [26].

X-ray absorption and high-pressure diffraction measurements were carried out at Sector 4-ID-D of the Advanced Photon Source. X-ray absorption was performed at ambient pressure and temperature, using single crystal Mo_3Sb_7 along with annealed Mo metal foil and MoO_2 and MoO_3 powders. For diffraction, 19.950 keV x rays were used in order to avoid the Mo K edge fluorescence. The methanol:ethanol 4:1 mixture was used as the pressure medium, and a piece of polycrystalline silver foil was included as a manometer at low temperature [26]. The ambient-pressure magnetization was measured using a superconducting quantum interference device (SQUID) magnetometer (Quantum Design Magnetic Property Measuring System) on a cubic shaped single crystal of 0.0138 g along the (1,1,0) direction and at both $T = 60$ and 6 K, bracketing the phase transition at T_S.

The pressure evolution of superconductivity in Mo_3Sb_7 was measured using ac magnetic susceptibility (Fig. 2). From 0 to 10 GPa, T_c slowly increases from 2.3 to 3 K with increasing P. Starting at 10 GPa, a new superconducting phase was observed with $T_c \sim 6$ K, a jump of a factor of two. This quantum phase transition between two superconducting states is clearly first order, with susceptibility manifesting two superconducting steps as a sign of phase coexistence over a wide pressure region [Fig. 2(a)]. As expected, an external magnetic field suppresses the superconducting transitions [Fig. 2(b)].

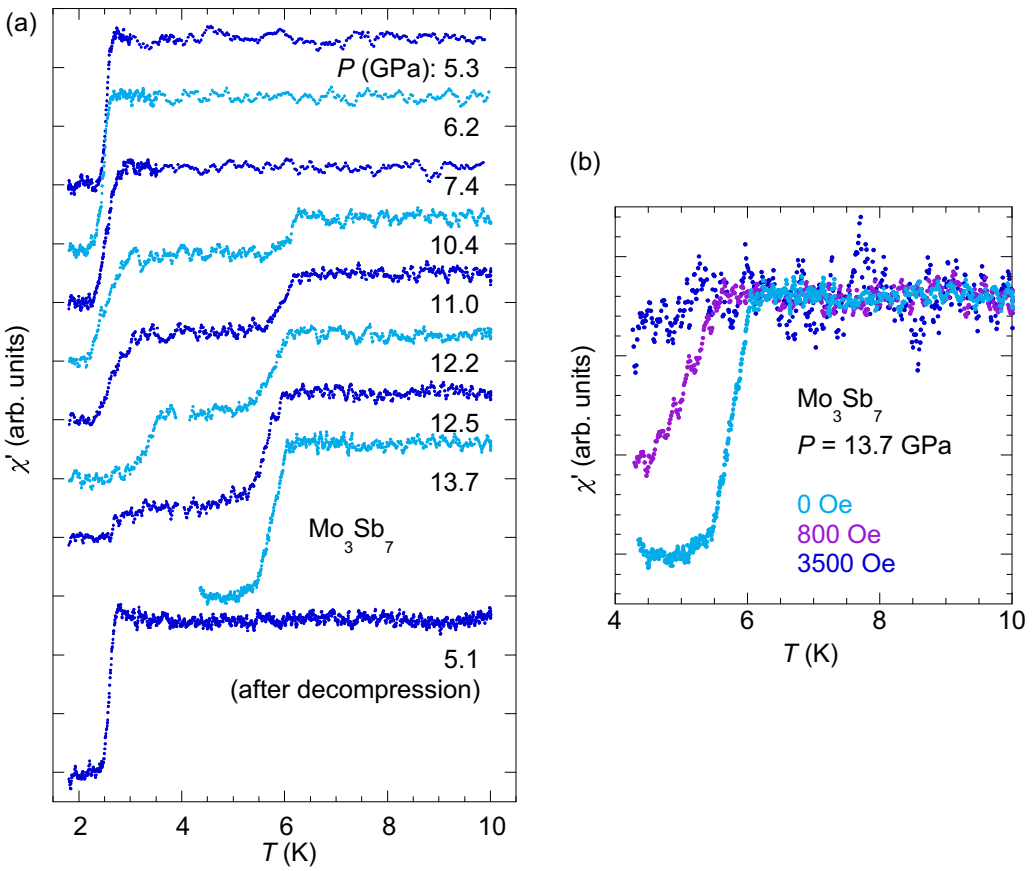

FIG. 2. (a) The ac magnetic susceptibility at the superconducting transition at a series of pressures P in Mo_3Sb_7. The two-step transitions indicate phase coexistence. (b) An applied magnetic field suppresses the superconductivity.

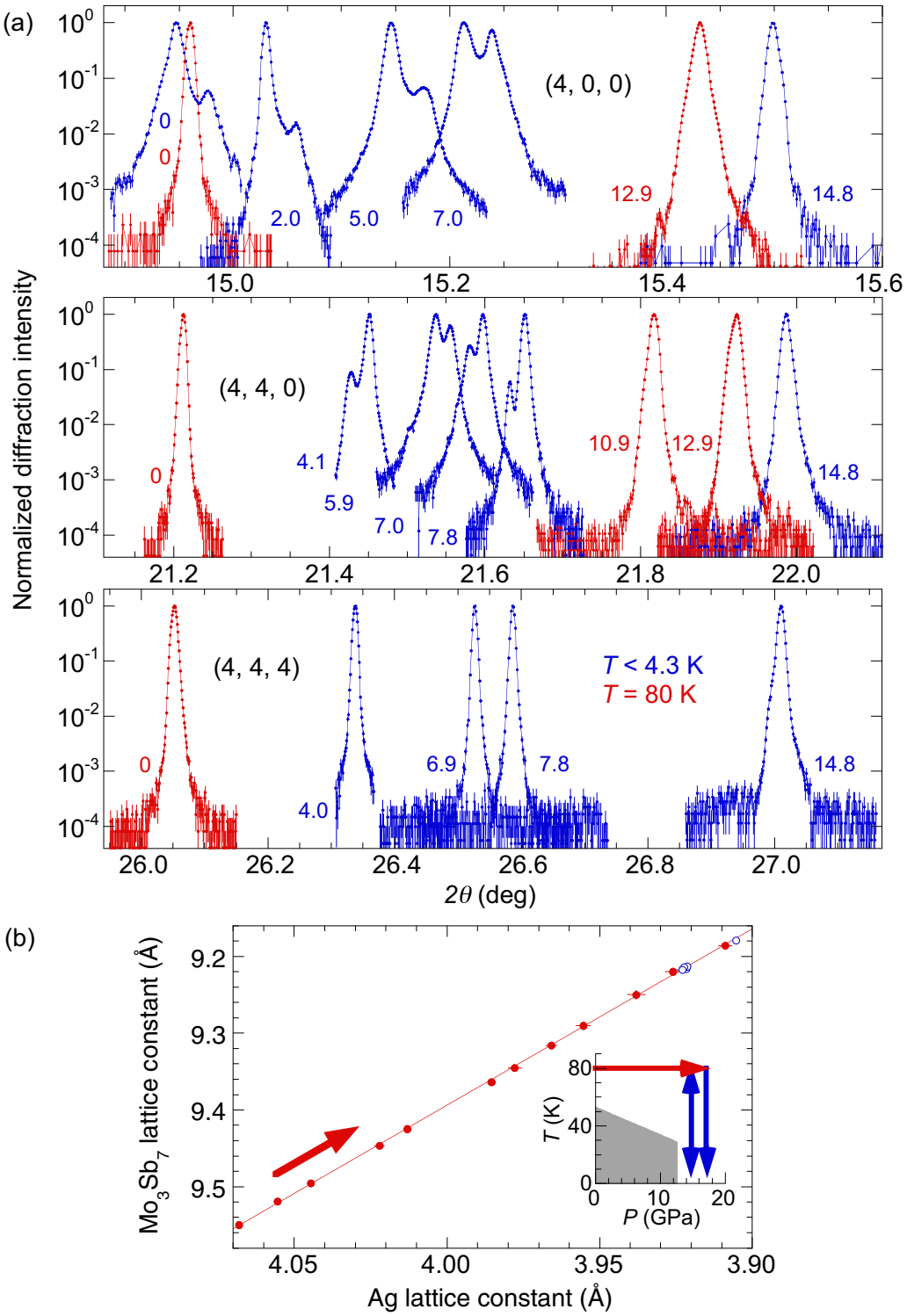

FIG. 3. Lattice symmetry and phase continuity. (a) Longitudinal ($\theta/2\theta$) scans of three lattice orders of Mo_3Sb_7, measured for various pressures (in units of GPa) at $T = 80$ K (red) or $T < 4.3$ K (blue). All scans are plotted on a logarithmic scale in order to show the symmetry state and to rule out the presence of minor phases. (b) The Mo_3Sb_7 lattice constant vs Ag lattice constant at each (P,T) point along the specified path in the inset. (Inset) Trajectory in the $P-T$ phase space for x-ray measurements. Mo_3Sb_7 remains in the same cubic phase throughout. The bulk modulus at 80 K is $B_0 = 111.5 \pm 0.8$ GPa .

Turning to structural information, the phase boundary $T_S(P)$ was tracked by macroscopic probes such as the electrical resistivity [27], where $T_S(P)$ is suppressed by increasing pressure (Fig. 1), but only slowly (~2.5 K/GPa), remaining well above zero out to 12 GPa. We performed a set of x-ray diffraction measurements to specify the evolution with P of the microscopic structure and associated lattice symmetries. Longitudinal diffraction line scans of various lattice orders such as (4, 0, 0), (4, 4, 0), and (4, 4, 4) at $T = 4$ K [Fig. 3(a)] indicate a lattice symmetry change from tetragonal at low

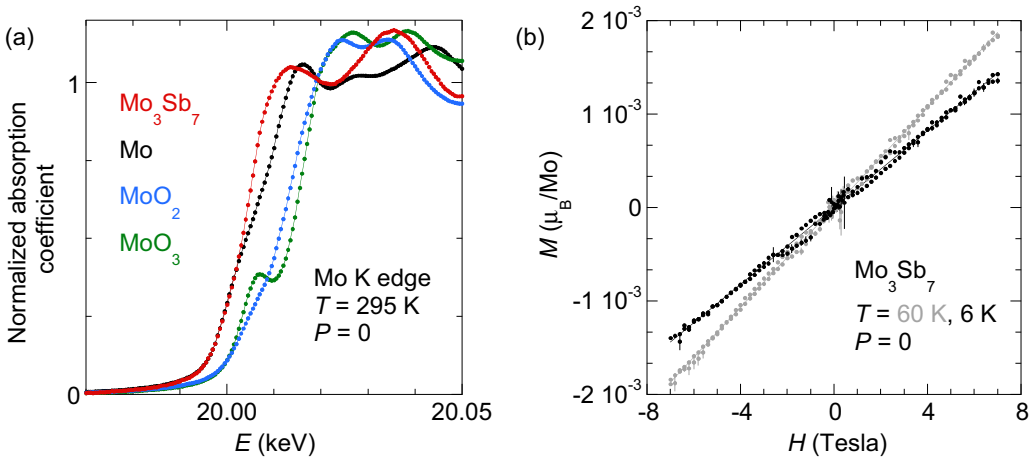

FIG. 4. Chemical and magnetic characteristics of Mo_3Sb_7. (a) X-ray absorption near-edge spectroscopy at ambient conditions for a comparison between four different Mo compounds of various valence conditions. (b) Magnetization measurements $M(H)$ at $T = 60$ K and 6 K, bracketing T_S at $P = 0$, indicate no magnetic hysteresis and no saturation up to $H = 7$ T.

pressure to cubic at high pressure. We examine in Fig. 3(b) the relationship between this high-pressure, low-temperature cubic phase and the ambient pressure, high-temperature cubic paramagnetic phase by traversing the $P - T$ phase diagram for $T > T_S$ out to $P = 17.1$ GPa. The lattice constants of both Mo_3Sb_7 and the silver manometer were measured at various (P, T) points along the path and then compared to each other. We find that $a_{Mo_3Sb_7}(P, T)$ vs $a_{Ag}(P,T)$ collapses onto a straight line throughout the trajectory. Hence the cubic phase of Mo_3Sb_7 at high P and low T and the cubic phase at $P = 0$ and $T > T_S$ are continuous, ruling out the separation that would result from a sudden unit cell collapse in an isostructural phase transition.

Given the continuous evolution of the ambient pressure paramagnet above $T_S = 53$ K to high pressure and low temperature, we might expect the spins in the high-pressure cubic phase of Mo_3Sb_7 to remain disordered. Spin fluctuations in Mo_3Sb_7 have been discussed in the literature based on the assumption of one $S = 1/2$ local moment per Mo site [10,11]. However, the existence of magnetic moments in Mo compounds strongly depends on its ionic state and local symmetry. For example, Mo^{4+} carries a moment of $S = 1$ in $1T - MoS_2$ but no moment in $2H - MoS_2$ due to a different splitting of the $4d$ orbitals by local symmetries [28]. In Ba_2YMoO_6 [29], a Mo^{5+} state leads to a localized $S = 1/2$ moment, which also was assumed for Mo_3Sb_7 [9]. The ionic state of Mo in Mo_3Sb_7 can be determined by x-ray absorption near-edge structure (XANES) measurements [30]. In the cubic phase of paramagnetic Mo_3Sb_7, there is only one unique Mo site in the unit cell [11], and the measured XANES K edge of Mo_3Sb_7 is very similar to that of pure Mo metal [Fig. 4(a)], lying 10–15 eV away from the K edge of both Mo^{4+} in MoO_2 and Mo^{6+} in MoO_3. This suggests that the Mo ions in Mo_3Sb_7 are close to charge neutral. They are also unlikely to have valence fluctuations like those displayed by highly ionized Re^{5+} ions in $Cd_2Re_2O_7$ [31].

We plot in Fig. 4(b) the dc magnetization, $M(H)$, at ambient pressure. It is linear and nonsaturating at both $T = 60$ and 6 K, above and below T_S, without hysteresis for applied fields between ± 7 T. Since Mo_3Sb_7 is cubic in the paramagnetic phase, no strong anisotropy of $M(H)$ is expected along the major crystalline axes. Here the nonsaturating $M(H)$ of Mo_3Sb_7 differs from the isothermal magnetization behavior of many magnetic Mo compounds. For ferromagnetic and paramagnetic MoS_2 [28,32] and ferromagnetic $GaMo_4S_8$ and $GaMo_4Se_8$ [33,34], $M(H)$ would saturate at relatively low fields, typically < 3 T. At $H = 7$ T, there is no saturation, and the measured moment is extremely small: $2 \times 10^{-3}\,\mu_B$/Mo. This small and unsaturated moment of Mo_3Sb_7 derived from $M(H)$ contrasts sharply from the magnetic moment deduced from the paramagnetic susceptibility, $\chi'(T)$. Fitting to a Curie-Weiss law for $230\,\text{K} < T < 700\,\text{K}$ yields a local moment of $1.56 \pm 0.10\,\mu_B$/Mo, consistent with $S = 1/2$ moment per Mo site [10,11]. The discrepancy between the values of the magnetic moment following from the magnetization at 7 T and fits to the magnetic susceptibility gives a Rhodes-Wohlfarth ratio ~500. This indicates that the Curie-Weiss behavior is due to band structure effects rather than localized spins [35]. Indeed the shortest Mo-Mo distance in Mo_3Sb_7 is 2.98 Å [11], a distance similar to the value of 2.73−2.9 Å in elemental Mo and ferromagnetic $GaMo_4S_8$ and $GaMo_4Se_8$ [33], where the overlap of $4d$ orbitals results in the electrons being considered as itinerant [33,34,36]. The combination of the valence state [Fig. 4(a)] and magnetization [Fig. 4(b)] measurements therefore permits us to conclude that the spins in Mo_3Sb_7 are highly itinerant and very small in magnitude. The magnetic nature of the tetragonal phase in Mo_3Sb_7 is consistent with paramagnetism [Fig. 4(b)]; the temperature dependence of the magnetic susceptibility at ambient pressure [10,11] could be due to a structural phase transition with no magnetic correlation, similar to that in $Cd_2Re_2O_7$ [31]. Hence we do not expect that the localized spin-dimer picture should be applicable to either phase of Mo_3Sb_7.

III. DISCUSSION

The superconducting transition in Mo_3Sb_7 lacks significant pressure dependence in either the tetragonal or cubic phase, leading to an abrupt doubling of the transition temperature at the phase boundary (Fig. 1). While the connection between

superconductivity and structural symmetry is particularly prominent, the crystal symmetry dependence of superconductivity is opposite to the typical expectation for spin-fluctuation-mediated superconductivity, which is believed to benefit more from a tetragonal structure than a higher symmetry cubic phase [4]. An increasing tetragonal distortion drives the system closer to the two-dimensional limit and hence enhances spin fluctuations via a diverging $\chi_m(\boldsymbol{q},\omega)$. This trend has been observed in heavy fermion superconductors; for example, T_c is significantly larger in tetragonal $CeRhIn_5$ than in cubic $CeIn_3$ [4]. Here in Mo_3Sb_7, T_c in the high-symmetry cubic phase doubles that in the low-symmetry tetragonal phase, while both structures are stable ground states. Symmetry considerations thus favor phonon-mediated superconductivity in Mo_3Sb_7 at high pressure.

Analogous to the original BCS formula in the weak coupling limit, T_c is expressed in McMillan's formula for intermediate phonon-coupling strength [22,37,38] as

$$T_c = \frac{\Theta}{1.45}\exp\left(-\frac{1.04\,(1+\lambda)}{\lambda-\mu^*(1+0.62\lambda)}\right), \qquad (1)$$

with the Debye temperature, Θ, dimensionless electron-phonon coupling constant, λ, and screened Coulomb potential, μ^*. While all three could potentially vary under pressure to account for the T_c evolution, both the constancy of the superconducting transition within each structural phase and its discontinuous nature in the phase coexistence region strongly suggest that the cause can be identified by comparing two structural phases of different symmetries at the same pressure. From calculations at ambient pressure [37], it is reasonable to assume that both Θ and μ^* are nearly identical in the tetragonal and cubic phases at the same pressure in the phase coexistence region. We therefore believe that the main influence on T_c should come from the electron-phonon coupling constant λ, with λ dependent on both electronic structure and the phonon dispersion spectrum [38]. The smoothly varying resistivity under pressure [27] indicates a continuously evolving electronic structure, consistent with estimated small difference between the tetragonal and cubic structures by theoretical calculation at ambient pressure [37]. Hence the origin of the doubled T_c most likely arises from details of the symmetry-dependent phonon dispersion [38]. This causes λ to grow from 0.55 at ambient pressure [22,37] to 0.75 in the cubic phase.

Spin fluctuations in general would disrupt a phonon-coupled superconductor by suppressing the value of λ [22] and thereby T_c. All suggested forms of singlet magnetic correlations (either long range antiferromagnetic order or spin-dimer pairs) in the tetragonal phase would introduce *reduced* singlet-type spin fluctuations as compared to fluctuations in the spin-disordered, high-pressure phase. This dearth of spin fluctuations in the tetragonal phase is consistent with the fact that $\rho(T)$ does not manifest $T^{3/2}$ behavior at ambient pressure [10,11,39]. If spin fluctuations would affect the phonon-mediated superconducting state in Mo_3Sb_7 [39], then $T_c(P)$ should be suppressed in the spin-disordered cubic high-pressure phase, while the experiments demonstrate the opposite.

IV. CONCLUSIONS

In summary, pressure enhances the superconducting transition temperature in Mo_3Sb_7 by a factor of two, accompanied by a first order phase transition from tetragonal to cubic lattice symmetry at low temperature. Direct x-ray diffraction results reveal that the high-pressure cubic phase continuously evolves from the paramagnetic phase at ambient pressure and is expected to be spin disordered. However, given the relatively small itinerant moments and weak spin fluctuation effects, we attribute the increase of T_c to a modified phonon density-of-states in the high-symmetry cubic structure. We are able to draw this conclusion because of the combination of magnetic, electronic, and structural measurements and the ability to tune different lattice symmetries with pressure. This general approach is necessary to parse the competition between different pairing mechanisms in materials with tendencies towards both magnetic and superconducting order.

ACKNOWLEDGMENTS

We thank J. Q. Yan and B. C. Sales for providing samples, J.-G. Cheng for communication of unpublished data, and M. Norman for enlightening discussions. The work at Caltech was supported by the U.S. Department of Energy Basic Energy Sciences Award No. DE-SC0014866. The high-pressure ac susceptibility measurements used shared facilities of the University of Chicago Materials Research Science and Engineering Center (National Science Foundation Grant No. DMR-1420709). The x-ray work at the Advanced Photon Source of Argonne National Laboratory was supported by the U.S. Department of Energy Basic Energy Sciences under Contract No. DE-AC02-06CH11357. The SQUID magnetometry measurements were performed at the Center for Nanoscale Materials of Argonne National Laboratory, a U.S. Department of Energy Office of Science User Facility, under Contract No. DE-AC02-06CH11357 with the assistance of B. Fisher. The work at Oak Ridge National Laboratory was supported by the U.S. Department of Energy, Office of Science, Basic Energy Sciences, Materials Sciences and Engineering Division.

[1] M. Imada, A. Fujimori, and Y. Tokura, Rev. Mod. Phys. **70**, 1039 (1998).
[2] Y. Feng, J. van Wezel, J. Wang, F. Flicker, D. M. Silevitch, P. B. Littlewood, and T. F. Rosenbaum, Nat. Phys. **11**, 865 (2015).
[3] L. C. Gupta, Adv. Phys. **55**, 691 (2006).
[4] P. Monthoux, D. Pines, and G. G. Lonzarich, Nature **450**, 1177 (2007).
[5] S. Yasuzuka and K. Murata, Sci. Technol. Adv. Mater. **10**, 024307 (2009).
[6] E. Fradkin, S. A. Kivelson, and J. M. Tranquada, Rev. Mod. Phys. **87**, 457 (2015).
[7] G. R. Stewart, Rev. Mod. Phys. **83**, 1589 (2011).
[8] L. Li, C. Richter, J. Mannhart, and R. C. Ashoori, Nat. Phys. **7**, 762 (2011).

[9] T. Koyama, H. Yamashita, Y. Takahashi, T. Kohara, I. Watanabe, Y. Tabata, and H. Nakamura, Phys. Rev. Lett. **101**, 126404 (2008).
[10] V. H. Tran, W. Miiller, and Z. Bukowski, Phys. Rev. Lett. **100**, 137004 (2008).
[11] J.-Q. Yan, M. A. McGuire, A. F. May, H. Cao, A. D. Christianson, D. G. Mandrus, and B. C. Sales, Phys. Rev. B **87**, 104515 (2013).
[12] D. J. Van Harlingen, Rev. Mod. Phys. **67**, 515 (1995).
[13] C. C. Tsuei and J. R. Kirtley, Rev. Mod. Phys. **72**, 969 (2000).
[14] F. Kidwingira, J. D. Strand, D. J. Van Harlingen, and Y. Maeno, Science **314**, 1267 (2006).
[15] W. Wu, J. Cheng, K. Matsubayashi, P. Kong, F. Lin, C. Jin, N. Wang, Y. Uwatoko, and J. Luo, Nat. Commun. **5**, 5508 (2014).
[16] H. Kotegawa, S. Nakahara, H. Tou, and H. Sugawara, J. Phys. Soc. Japn. **83**, 093702 (2014).
[17] J.-G. Cheng, K. Matsubayashi, W. Wu, J. P. Sun, F. K. Lin, J. L. Luo, and Y. Uwatoko, Phys. Rev. Lett. **114**, 117001 (2015).
[18] Y. Wang, Y. Feng, J.-G. Cheng, W. Wu, J. L. Luo, and T. F. Rosenbaum, Nat. Commun. **7**, 13037 (2016).
[19] J.-Q. Yan, M. A. McGuire, A. F. May, D. Parker, D. G. Mandrus, and B. C. Sales, Phys. Rev. B **92**, 064507 (2015).
[20] C. Candolfi, B. Lenoir, A. Dauscher, J. Hejtmánek, E. Šantavá, and J. Tobola, Phys. Rev. B **77**, 092509 (2008).
[21] R. Khasanov, P. W. Klamut, A. Shengelaya, Z. Bukowski, I. M. Savić, C. Baines, and H. Keller, Phys. Rev. B **78**, 014502 (2008).
[22] B. Wiendlocha, J. Tobola, M. Sternik, S. Kaprzyk, K. Parlinski, and A. M. Oleś, Phys. Rev. B **78**, 060507 (2008).
[23] C. Candolfi, B. Lenoir, A. Dauscher, J. Hejtmánek, and J. Tobola, Phys. Rev. B **79**, 235108 (2009).
[24] Y. Feng, D. M. Silevitch, and T. F. Rosenbaum, Rev. Sci. Instrum. **85**, 033901 (2014).
[25] A. Palmer, D. M. Silevitch, Y. Feng, Y. Wang, R. Jaramillo, A. Banerjee, Y. Ren, and T. F. Rosenbaum, Rev. Sci. Instrum. **86**, 093901 (2015).
[26] Y. Feng, R. Jaramillo, J. Wang, Y. Ren, and T. F. Rosenbaum, Rev. Sci. Instrum. **81**, 041301 (2010).
[27] G. Z. Ye, J.-G. Cheng, J.-Q. Yan, J. P. Sun, K. Matsubayashi, T. Yamauchi, T. Okada, Q. Zhou, D. S. Parker, B. C. Sales, and Y. Uwatoko, Phys. Rev. B **94**, 224508 (2016).
[28] S. Yan, W. Qiao, X. He, X. Guo, L. Xi, W. Zhong, and Y. Du, Appl. Phys. Lett. **106**, 012408 (2015).
[29] M. A. de Vries, A. C. Mclaughlin, and J.-W. G. Bos, Phys. Rev. Lett. **104**, 177202 (2010).
[30] S. P. Cramer, T. K. Eccles, F. W. Kutzler, K. O. Hodgson, and L. E. Mortenson, J. Am. Chem. Soc. **98**, 1287 (1976).
[31] M. Hanawa, Y. Muraoka, T. Tayama, T. Sakakibara, J. Yamaura, and Z. Hiroi, Phys. Rev. Lett. **87**, 187001 (2001).
[32] S. Tongay, S. S. Varnoosfaderani, B. R. Appleton, J. Wu, and A. F. Hebard, Appl. Phys. Lett. **101**, 123105 (2012).
[33] V. Shamrai, H. Mädge, T. Mydlarz, and G. Leitus, J. Low Temp. Phys. **49**, 123 (1982).
[34] A. K. Rastogi, A. Berton, J. Chaussy, R. Tournier, M. Potel, R. Chevrei, and M. Sergent, J. Low Temp. Phys. **52**, 539 (1983).
[35] T. Moriya, *Spin Fluctuations in Itinerant Electron Magnetism* (Springer-Verlag, Berlin,1985).
[36] W. M. Lomer, Proc. Phys. Soc. (London) **80**, 489 (1962).
[37] B. Wiendlocha and M. Sternik, Intermetallics **53**, 150 (2014).
[38] W. L. McMillan, Phys. Rev. **167**, 331 (1968).
[39] C. Candolfi, B. Lenoir, A. Dauscher, C. Bellouard, J. Hejtmánek, E. Šantavá, and J. Tobola, Phys. Rev. Lett. **99**, 037006 (2007).